Ferrite-based Materials for Removal Heavy Metals

Ahmad Anwar Hassan[1], Samir. A. Abdel-Latif[2], Mohammed Eid M. Ali[3*]

[1]Central Laboratories of the Egyptian Mineral Resources Authority, Dokki, Cairo, Egypt

[2]Chemistry Department, Faculty of *Science, Helwan University, Cairo, Egypt*

[3]Water Pollution Research Department, National Research Center, El-Bouthous, Dokki, Cairo, Egypt, P.O. 12622

**Corresponding author: Mohammed Eid M. Ali, e-mail: alienv81@yahoo.com, mailing address: [3]Water Pollution Research Department, National Research Center, El-Bouthous, Dokki, Cairo, Egypt, P.O. 12622/ Tel: 00201008457583*

Abstract

Spinel nickel ferrite was synthesized by low temperature regime in which no calcination temperature is induced. The as-prepared nickel ferrite is used for treatment hexavalent chromium Cr (VI) and pentavalent arsenic As (V) ions from wastewater by adsorption technique. Cr (VI) ions were removed by maximum efficiency reached to 60% after 90 minutes at pH 5, 2 g/L of ferrite dose and concentration of Cr (VI) ions is 25 mg/L. As (V) ions were treated by maximum efficiency reached to 75% after 90 minutes at pH 5, dose of ferrite of 1 g/L and concentration of As (V) ions is 25 mg/L. kinetic and isothermal study of adsorption of Cr (VI) and As (V) ions onto nickel ferrite surface indicates that sorption is favorable and spontaneous. Cr (VI) ions adsorption follows Pseudo first order kinetics reaction while As (V) ions adsorption follows Pseudo second order kinetics reaction. Conclusively, nickel ferrite has more uptakes for As (V) rather than Cr (VI).

Keywords

Nickel Ferrite, hexavalent chromium, pentavalent arsenic, adsorption, wastewater

1. Introduction

Scientific advancement and industrialization have been both beneficial and problematic for the environment and to human populations. Problems associated with water are particularly notable. Water is an essential source for maintaining life on this planet. Metal ions are one of the most concerning of the toxic pollutants that are

released into aqueous environments. With rapidly increasing industrialization and increasing human needs, the global production of products containing toxic metal ions has increased, and the amount of toxic metal-containing wastewater released by industries has also increased. Chromium and its compounds are broadly used in plating, leather tanning, metal finishing, photography, and nuclear power plants (Ajmal et al., 2001; Selvarajet et al., 2003). Hexavalent chromium concentrations are ranged from tens to hundreds of mg/L in the effluents produced from these industries. Chromates (CrO_4^{2-}), dichromates ($Cr_2O_7^{2-}$), and bichromates ($HCrO_4^-$) are hexavalent chromium forms of oxyanions in wastewaters. Because of its high solubility, hexavalent chromium is more toxic to living organisms than trivalent chromium (Brown et al., 2000).

Arsenic has toxic and carcinogenic characteristics as pollutant present in drinking water. Pentavalent arsenic is predominant in the form of oxyanions such as H_3AsO_4, $H_2AsO_4^-$ and $HAsO_3^{2-}$ (Mohan and Pittman, 2007). Chronic exposure to arsenic contaminated water can cause serious medical complications such as loss of appetite, cancer of skin, lungs and bladder (Mandal and Suzuki, 2002). Due to its hazardous effect, removal of chromium and arsenic from industrial wastewater has lately gained a lot of attention. Several studies have been performed on the study of magnetically treated adsorbents and their capability to remove chromium and arsenic from wastewater. Spinel ferrites used as adsorbents in water treatment to treat toxic contaminants from aqueous environment.

Spinel nickel ferrite is one of the most important ferrite materials, has been broadly studied due to its application in many fields, such as catalysts, ferrofluids gas sensors, magnetic materials and microwave devices (Houlding et al., 2013; Benrabaa et al., 2012; Al-Mayman and Al-Zahrani, 2003). The outstanding magnetic and electrical properties of nickel ferrite depend on the nature, the charges, and the distribution of metal ions into its crystal lattice (Dixit et al., 2010). Spinel nickel ferrite is considered good adsorbent for heavy metal removal because of its high surface-to-volume ratio, tunable size and shape, and tunable magnetic property (Kang et al., 2015).

This work is based on preparation of spinel nickel ferrite by facile method as active adsorbent for wastewater treatment. Hexavalent chromium Cr (VI) and pentavalent arsenic As (V) were removed by as-prepared nickel ferrite from wastewater as examples of inorganic pollutants.

2. Experimental

2.1. Reagents, apparatus and preparation of synthetic wastewater

Determinations of chromium, arsenic concentration and nickel ferrite by using inductive coupled plasma optical emission spectroscopy instrument (ICP-OES) model (Agilent-720 series). A WTW digital pH meter model 525 was used for the pH adjustments. Shaker was also used for mixing the samples with sorbent. Single component stock solutions of 1000 mg/L Cr (VI) and As (V) were prepared by dissolving appropriate amount of potassium chromate K_2CrO_4 (Merck) in deionized water for preparation Cr (VI) ions and arsenic pentaoxide As_2O_5 (Merck) in deionized water for preparation As (V) ions. Dilution was used for preparation the required concentration for the various steps of the investigation. Hydrochloric acid HCl (Merck) 1% (V/V) and/or sodium hydroxide NaOH (Merck) were used for pH adjustment of the synthetic wastewater.

2.2. Preparation and characterization of nickel ferrite

Nickel ferrite nanoparticles were prepared by the following procedures. $FeCl_3.6H_2O$ solution and $NiCl_2.6H_2O$ solution are mixed in deionized water with mole ratio 2:1 for Fe^{3+}/ Ni^{2+} and are magnetically stirred. Ammonia solution (25%) was added slowly into the mixture solution until pH＝9.5－10, under vigorous stirring. After the resulting mixture was kept boiling and refluxing for 2 h under vigorous stirring, $NiFe_2O_4$ nanoparticles were synthesized. Finally, the as-prepared $NiFe_2O_4$ nanoparticles were washed with deionized water and redispersion for four times. Furthermore, the phase structure was identified at room temperature with using Phillips X-ray diffractometer model X′Pert PRO using Cu Kα targets at 50 kV and 40 mA. The XRD patterns were obtained by two scanning modes. The fast scanning, for identification, was carried out between $2\theta = 2°$ and 60° at speed of 0.02°/sec.

2.3. General adsorption procedure

Batch adsorption experiments were carried out by shaking of 100 mL conical flasks containing different doses of nickel ferrite in different concentrations of single component solutions of Cr (VI) and As (V) ions at different pHs, the pH of the solutions was adjusted by adding HCl or NaOH solution. After stirring at a constant temperature at 298 K for different times, the solid/liquid phases were separated by filtration using membrane filter 0.45 µm. Then the concentration of Cr (VI) and As

(V) ions in filtrate was detected by inductive coupled plasma instrument. The removal efficiency was calculated based on the following equation:

$$\text{Removal efficiency } (\%) = \frac{C_o - C_e}{C_o} \text{ x } 100 \qquad \text{Eq. (1)}$$

Where C_o and C_e are the initial and the equilibrium concentrations of metal ion in solution phase, respectively. Kinetic experiments were performed on 50 mg/L of metal ion with nickel ferrite dose of 1 g/L at temperature 298 K and pH 5. On regular time intervals, suitable aliquots were taken where upon the metal ion concentration was determined. The rate constants were calculated using the conventional rate expression. Adsorption isotherm studies were carried out with initial concentrations of metal ion varying from 25 to 200 mg/L, the amount of sorbent was kept constant and the experimental temperatures were controlled at 298 K.

3. Results and Discussion

3.1. Effect of pH

The pH plays a very important role in the sorption of heavy metals, since it affects the surface charge of the adsorbent and the metal species present in the solution. The influence of the initial pH of Cr (VI) and As (V) solutions on the removal efficiency has been evaluated under the following conditions; Single component solutions of Cr (VI) and As (V) with initial concentration 20 mg/L, 1.0 g/L of nickel ferrite dose, 200 rpm agitation speed, 90 min contact time and pH ranging from 3 to 11. The effect of pH on the removal efficiency is illustrated in Fig 1. The removal efficiency of Cr (VI) ions increases from 18.4% at pH 11 to 53.4% at pH 5, also the removal efficiency of As (V) ions increases from 33.6% at pH 11 to 75.1% at pH 5. Notably, adsorption of Cr (VI) and As (V) ions on nickel ferrite surface increased with decrease in pH of metal solution. The point of zero charge of nickel ferrite is 6.7 so the surface of adsorbent will be positively charged at lower pH due to adsorption of hydrogen ions on the surface of adsorbents, at the same time, metals will be negative charged as they exist in the anion form so it will be adsorbed strongly at lower pH. Meanwhile, at higher pH value, surface of nickel ferrite is negatively charged, and repel with negatively charged anions of chromium and arsenic molecules and removal efficiency is suppressed as well.

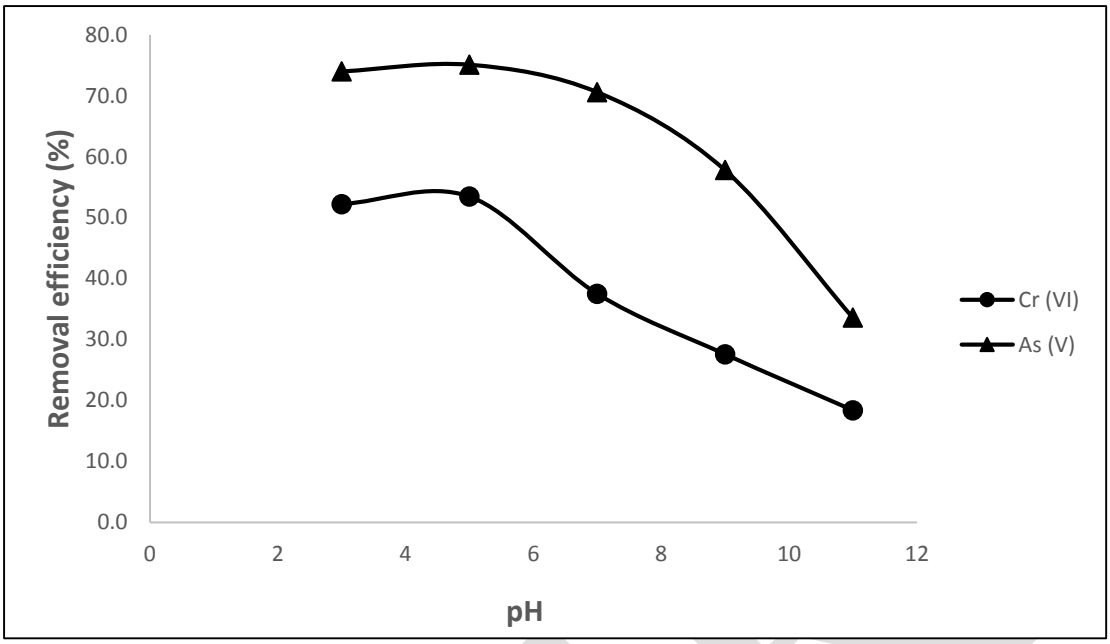

Fig. 1 Effect of pH on the removal efficiency of Cr (VI) and As (V) ions on nickel ferrite

3.2. Effect of the sorbent dose

Single component solutions of Cr (VI) and As (V) with initial concentration 50 mg/L mixed at 200 rpm with 0.25, 0.5, 1.0, 1.5 and 2.0 g/L of nickel ferrite for interaction time 90 minutes at pH 5. The obtained results in Fig. 2 showed that Cr (VI) removal efficiency increased from 9.6% at 0.25 g/L of nickel ferrite dose to 36% at 2.0, also As (V) removal efficiency increased from 7.8% at 0.25 g/L of nickel ferrite dose to 52.6% at 2.0 g/L of nickel ferrite dose. Firstly, the adsorption rate of metal enhanced with the nickel ferrite amount, whilst the more amount of nickel ferrite give a higher surface area and more active sites for adsorption. In case of adsorption of As (V), the over amount of sorbent in the solution may lead to slight increase adsorption rate (ca: 6%) this owe to agglomeration that diminishes the adsorption because active sites for adsorption are not completely occupied. From economic point of view, 2 g/L and 1.5 g/L are chosen as optimal dose for Cr (VI) and As (V) adsorption, respectively.

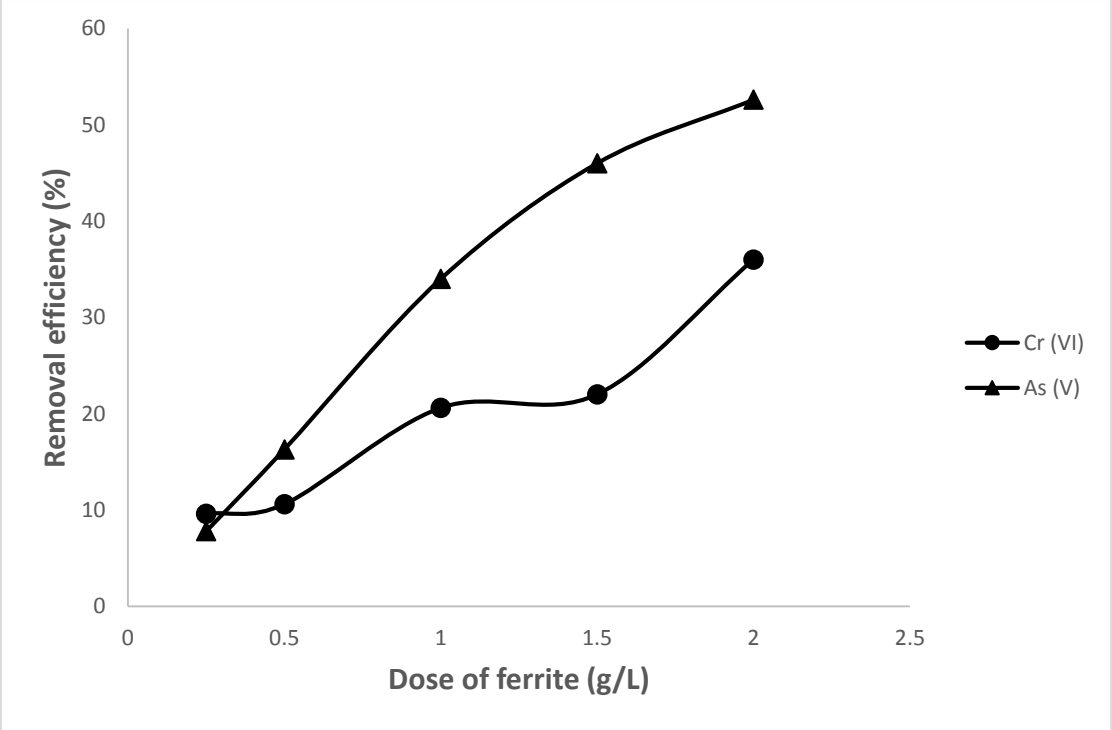

Fig. 2 Effect of adsorbent dose on the removal efficiency of Cr (VI) and As (V) ions on nickel ferrite

3.3. Effect of contact time

To determine the required time for obtaining equilibrium, single component solutions of Cr (VI) and As (V) with initial concentration 50 mg/L mixed at 200 rpm with 1.0 g/L of nickel ferrite for interaction at pH 5. The results are illustrated in Fig. 3. For Cr (VI) ions removal efficiency is progressively increased with time and equilibrium was achieved after 120 minutes with 36% of removal at 298 K. Removal efficiency of As (V) ions increased with increasing time. Equilibrium was reached with 47% of removal at 298 K after 120 minutes.

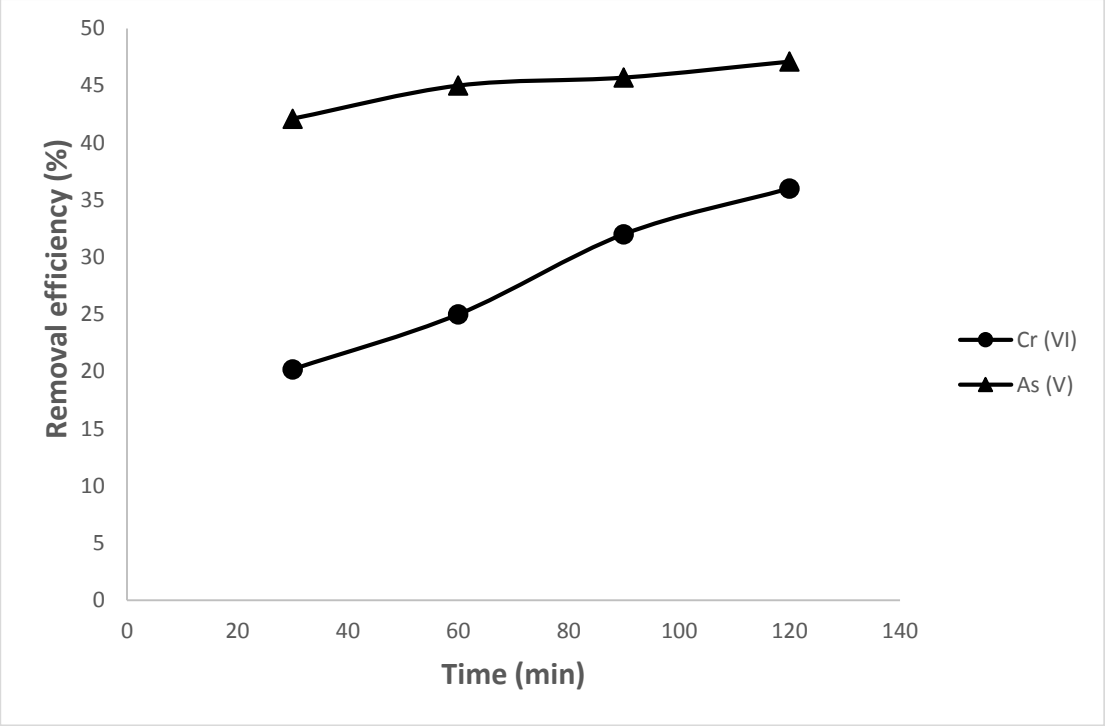

Fig. 3 Effect of contact time on the removal efficiency for Cr (VI) and As (V) ions on nickel ferrite

3.4. Effect of initial metal ion concentration

Single component solutions of Cr (VI) and As (V) ions with different concentrations of 25, 50, 75, 100 and 200 mg/L were mixed at 200 rpm with 2 g/L of nickel ferrite for equilibrium time 90 min at pH 5. The obtained results in Fig. 4 clarified that for Cr (VI) ions the removal efficiency decreased from 60% at initial concentration 25 mg/L to 12% at 200 mg/L of initial concentration of Cr (VI) ions. For As (V) ions the removal efficiency decreased from 61% at initial concentration 25 mg/L to 24.7% at 200 mg/L of initial concentration of As (V) ions. It is obvious that removal efficiency increases with decreasing of initial metal ion concentration as increase in metal ion concentration results in lower probability of collision with active surface sites of nickel ferrite so removal of metal ions decrease.

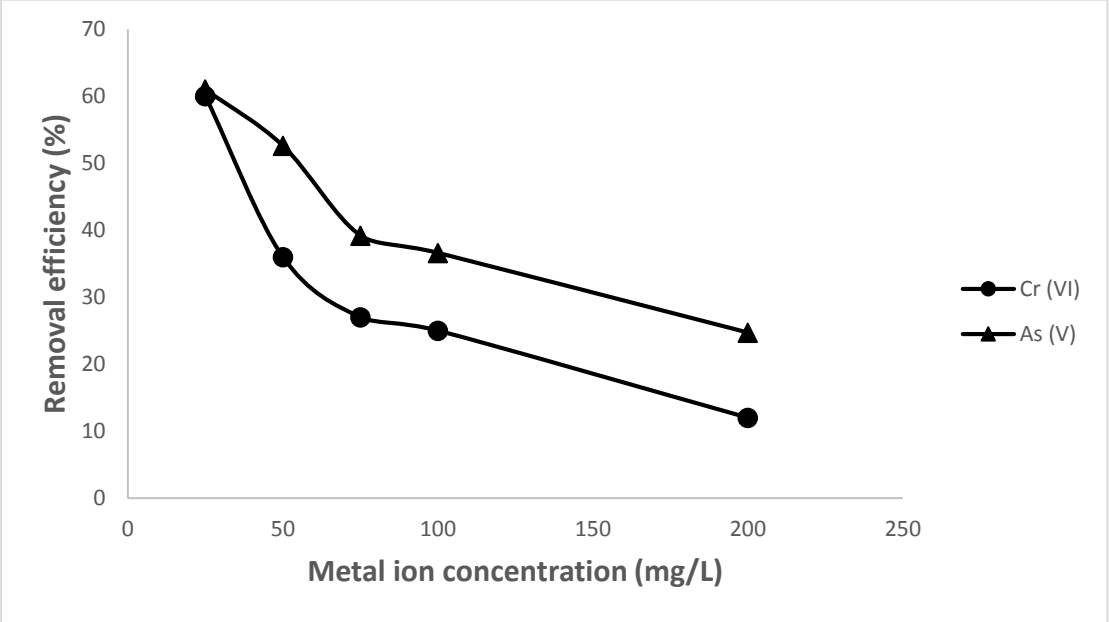

Fig. 4 Effect of initial metal ion concentration on the removal efficiency for Cr (VI) and As (V) ions on nickel ferrite

3.5. Adsorption kinetics

In order to gain a better understanding of the adsorption process mechanism of Cr (VI) and As (V) ions by nickel ferrite, the following kinetic models have been used to test the experimental data.

3.5.1. Pseudo-first-order model

This kinetic model can be expressed as follows (Azizian, 2004):

$$\ln(q_e - q_t) = \ln q_e - K_1\, t \qquad \text{Eq. (2)}$$

Where q_e and q_t are the amount of metal ion adsorbed on the adsorbent (mg/g) at equilibrium and at time t, respectively, and K_1 is the rate constant of the first-order adsorption (min^{-1}). By plotting ln (q_e - q_t) versus t, that give a linear relationship, the first order constant (K_1) and equilibrium adsorption capacity (q_e) were determined from the slope and intercept of the plot, respectively. The values of correlation coefficient (R^2), K_1 and q_e calculated from linear pseudo first-order equation have been presented in Table 1. For Cr (VI), the correlation coefficient (R^2) is relatively high, its value is 0.98. The calculated q_e value obtained from the equation is 18.5 mg/g which is closed to experimental q_e value (18 mg/g). It is noticeable that calculated q_e value is in good agreement with experimental q_e value.

This finding suggests that the adsorption process follow the pseudo first-order adsorption rate expression. For As (V), the value of correlation coefficient (R^2) is low (0.62), the calculated q_e value (2.3 mg/g) obtained from the equation is too low compared with experimental q_e value (23.5 mg/g) and doesn't agree with it so the adsorption of As (V) ions on nickel ferrite doesn't follow the pseudo first-order adsorption rate expression.

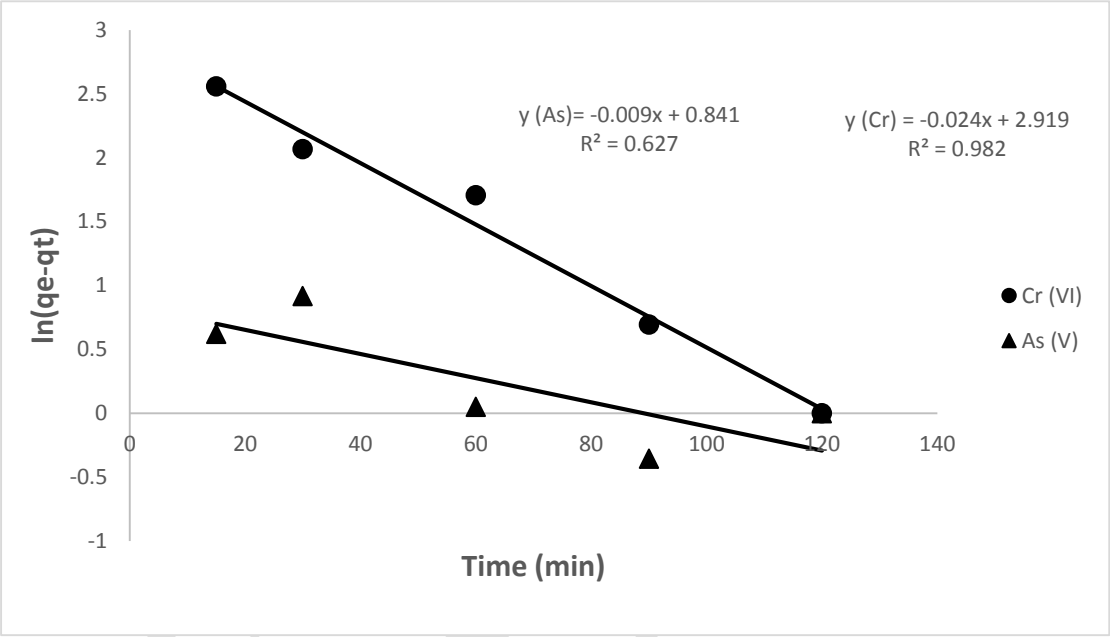

Fig. 5 Pseudo first order plot for adsorption of Cr (VI) and As (V) ions onto nickel ferrite

3.5.2. Pseudo-second-order model

The adsorption data have been simulated by pseudo-second-order model, which is expressed by the following equation (Azizian, 2004):

$$\frac{t}{q_t} = \frac{t}{q_e} + \frac{1}{k_2 {q_e}^2} \qquad \text{Eq. (3)}$$

The q_e and the second order constant K_2 were determined experimentally from the slope and intercept of the linear plot t/q_t versus t and presented in Table 1 along with the corresponding correlation coefficient (R^2). For Cr (VI), the correlation coefficient (R^2) is 0.98 although it is high but the calculated q_e value (25.1 mg/g) obtained from the equation is higher compared with experimental q_e value (18 mg/g) and doesn't agree with it (Table 1). So adsorption of Cr (VI) ions onto nickel ferrite surface does

not obey Pseudo-second-order model. For As (V), the correlation coefficient (R^2) is 0.99 and the calculated q_e value obtained from the equation is 24.2 mg/g which is close to experimental q_e value (23.5 mg/g) (Table 1). Hence, the adsorption system of ions obeys the pseudo-second-order model which describes the chemical sorption and thus some type of chemical reaction is considered to take place that includes valence forces with the exchange of ions or the formation of covalent bonds (Malamis and Katsou, 2013).

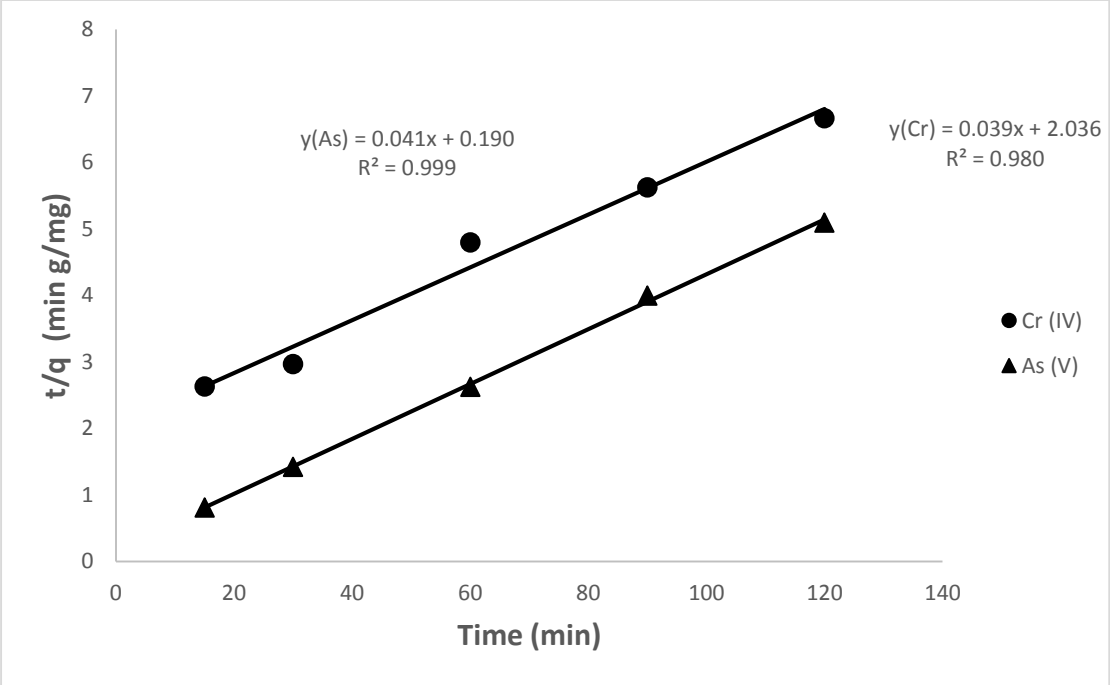

Fig. 6 Pseudo second order plot for adsorption of Cr (VI) and As (V) ions onto nickel ferrite

3.5.3. Weber–Morris kinetic model

The mathematical expression of Weber–Morris kinetic model can be represented as follows (Weber and Morris, 1963):

$$q_t = k_d t^{1/2} + I \qquad \text{Eq. (4)}$$

K_d is the rate constant for intra-particle diffusion. I values give an idea about the thickness of the boundary layer. Hence, the smaller the intercept, the lower the boundary layer effect will be (Khenifi et al., 2009).

In Fig. 7 a plot of q_t versus $t^{1/2}$gives a linear relationship which indicated that intraparticle diffusion is involved in the adsorption process.

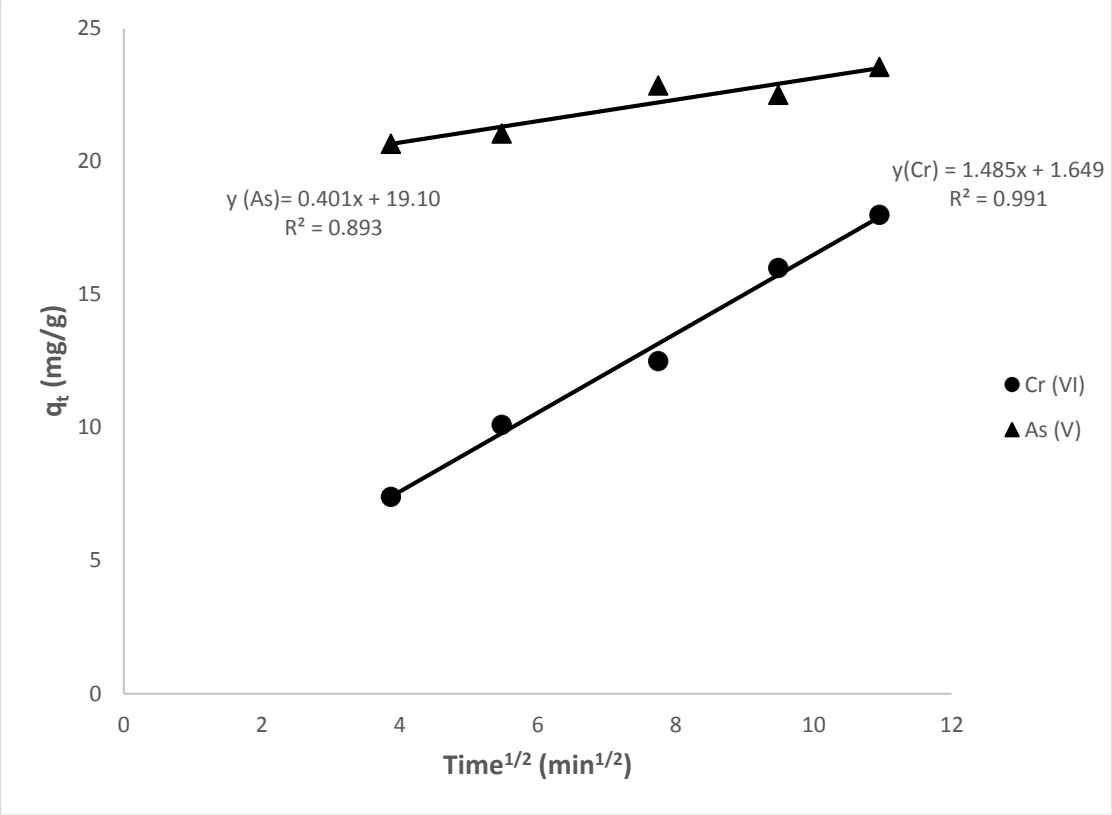

Fig. 7 Weber–Morris plots for adsorption of Cr (VI) and As (V) ions onto nickel ferrite

3.5.4. Boyd plot

The Boyd plot profile was obtained by plotting the calculated B_t versus time t. The B_t is expressed by the following equation:

$$B_t = -\ln\left(1 - \frac{q_t}{q_e}\right) - 0.4977 \qquad \text{Eq. (5)}$$

Fig. 8 illustrate time profile of the calculated B_t values. The linear relationship provides useful information to differentiate between external mass transfer and intraparticle diffusion controlled mechanism of adsorption. It was noticed that the plots did not pass through the origin, indicating that external mass transfer is involved in the entire adsorption process (Gupta et al., 2008).

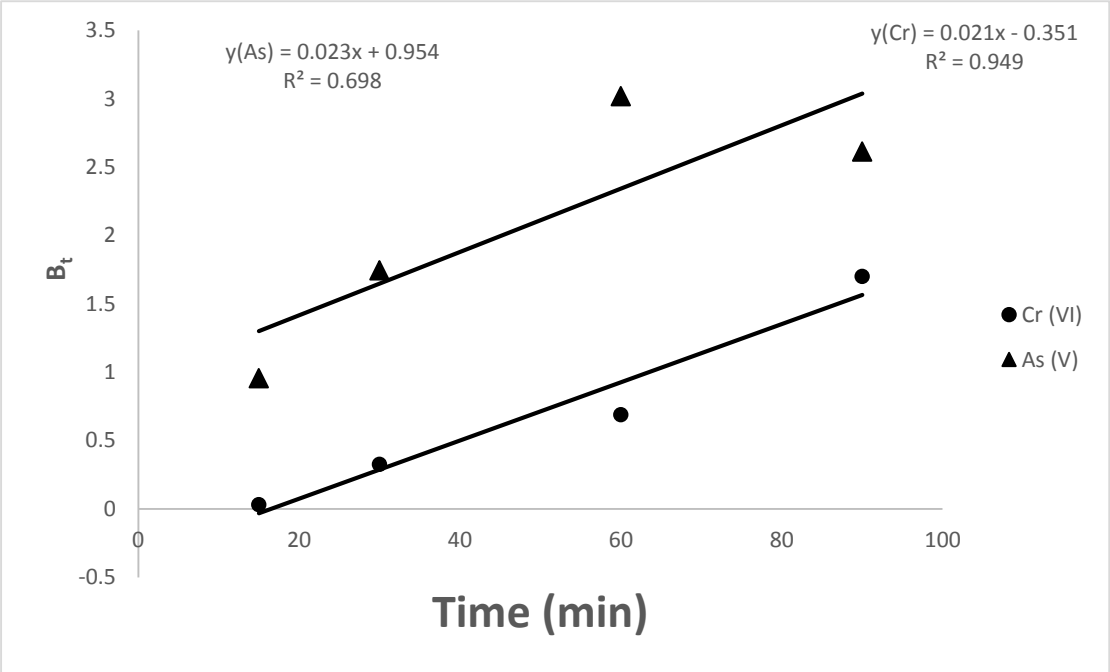

Fig. 8 Plot of B_t versus time for the adsorption of Cr (VI) and As (V) ions onto nickel ferrite

Table 1 Kinetic parameters of Cr (VI) and As (V) adsorption over nickel ferrite

Metal Ion	$q_{e(exp)}$ (mg/g)	Pseudo-first-order			Pseudo-second-order			Weber–Morris kinetic		
		qe(cal) (mg/g)	K1 (min^{-1})	R^2	qe(cal) (mg/g)	K2 (g/(mg min))	R^2	K_d	I	R^2
Cr (VI)	18	18.5	0.024	0.98	25.1	0.0007	0.98	1.48	1.64	0.99
As (V)	23.5	2.3	0.009	0.62	24.3	0.008	0.99	0.4	19.1	0.89

3.6. Adsorption isotherms

The adsorption isotherm represents the equilibrium relationship between the adsorbate concentration in the liquid phase and that on the adsorbents surface at given condition. The sorption data have been subjected to different sorption isotherms, namely, Langmuir, Freundlich, Temkin, Dubinin–Radushkevich and Flory–Huggins models.

3.6.1. Langmuir isotherm model

The linearized Langmuir isotherm model, which is valid for monolayer adsorption onto a surface with finite number of homogenous sites, is expressed as follows (Langmuir, 1916):

$$\frac{c_e}{q_e} = \frac{1}{k_L q_{max}} + \frac{c_e}{q_{max}} \quad \text{Eq. (6)}$$

Where q_{max} is the maximum monolayer adsorption (mg/g), C_e is the equilibrium concentration of metal ions (mg/L), q_e is the amount of metal ions adsorbed per unit weight of nickel ferrite at equilibrium concentration (mg/g) and K_L is the Langmuir constant related to the affinity of binding sites (L/mg). By plotting of C_e/q_e against C_e the Langmuir isotherm constants were determined. The obtained isothermal constants and the correlation coefficients are presented in Table 2. For Cr (VI), the plot yield straight line with R^2=0.99 which means that adsorption equilibrium obeys Langmuir equation. For As (V), the correlation coefficient (R^2) is 0.98 which indicates that adsorption equilibrium also obeys Langmuir model.

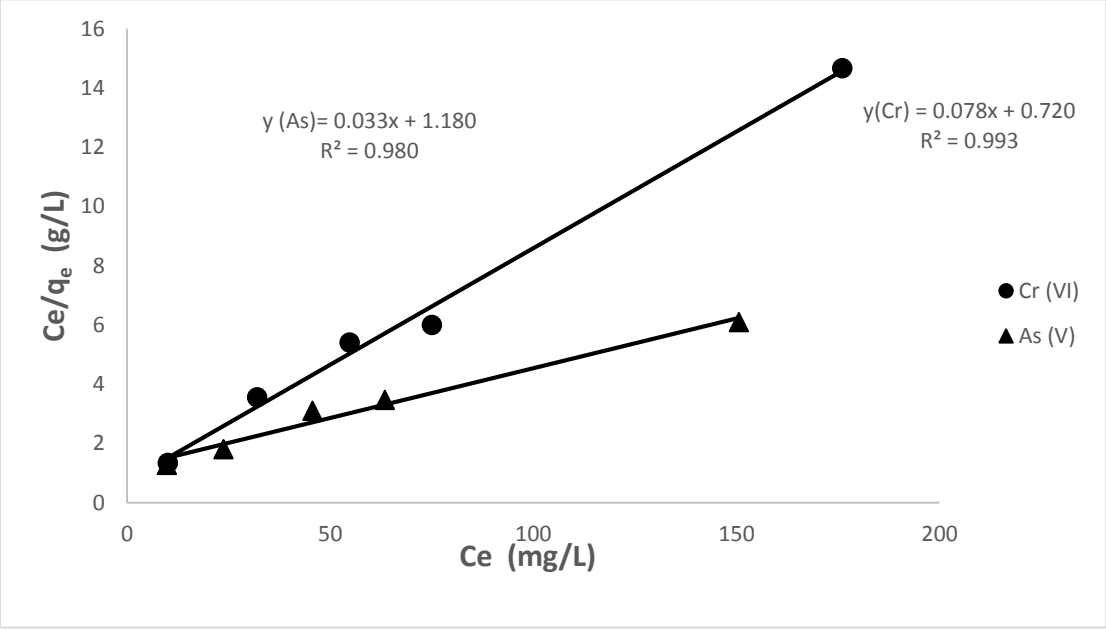

Fig. 9 Langmuir plot of Cr (VI) and As (V) ions adsorption on nickel ferrite

The essential characteristics of the Langmuir isotherms can be expressed by means of RL, a dimensionless constant referred to as the separation factor or equilibrium parameter (Wan-Ngah et al., 2004). RL is calculated using the following equation:

$$R_L = \frac{1}{1+ K_L C_0} \quad \text{Eq. (7)}$$

Where C_o is the initial metal ions concentration (mg/L) and K_L is the Langmuir adsorption equilibrium constant (L/mg). The R_L parameter is considered as a more reliable indicator of the adsorption. It indicates the shape of the isotherm to be either; unfavorable (R_L> 1), linear (R_L = 1), favorable (0 <R_L< 1) or irreversible (R_L = 0). In the present investigation for both Cr (VI) and As (V), the calculated values of R_L were found in the range 0 <R_L< 1, confirm the favorable uptake of Cr (VI) and As (V) process. It ranged between 0.06-0.26 for Cr (VI) and 0.11- 0.58 for As (V).

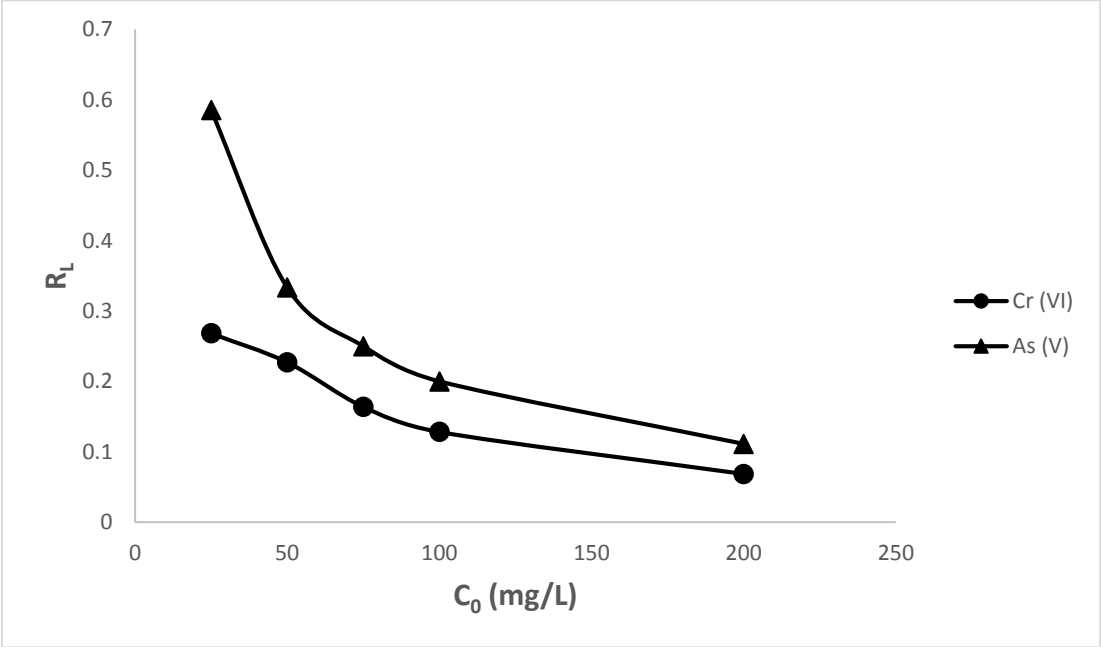

Fig. 10 Separation factor R_L versus initial concentration for the adsorption of Cr (VI) and As (V) ions onto nickel ferrite

3.6.2. Freundlich isotherm model

The linearized Freundlich model can be represented as following (Freundlich, 1906):

$$\ln q_e = \ln k_F + \frac{\ln C_e}{n} \quad \text{Eq. (8)}$$

Where K_F and n are Freundlich constants indicating the sorption capacity (mg/g) and intensity, respectively. By plotting of $\ln q_e$ versus $\ln C_e$ the Freundlich isotherm constants were determined at 298 K. The obtained isothermal constants and the correlation coefficients are presented in Table 2. The correlation coefficient (R^2) for

Cr (VI) ions is 0.86 which is less fitted with Freundlich isotherm model. For As (V) the correlation coefficient (R^2) is 0.97. Therefore, the Freundlich isotherm fits better.

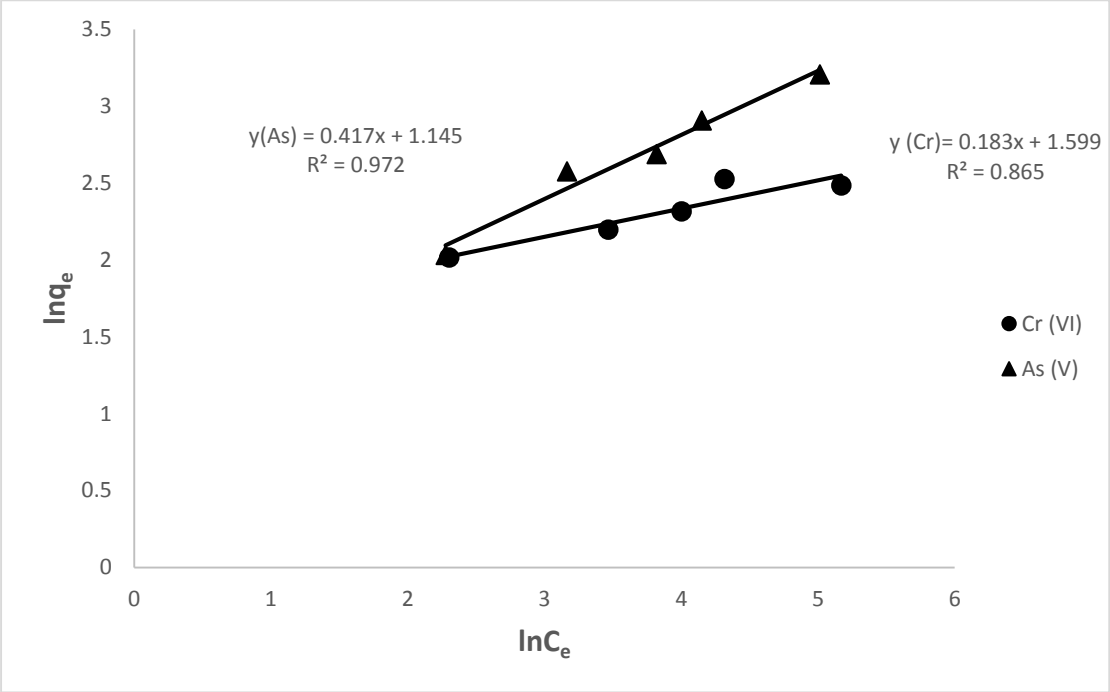

Fig. 11 Freundlich plot of Cr (VI) and As (V) ions adsorption on nickel ferrite

3.6.3. Temkin isotherm model

The linearized Temkin equation is given by the following equation (Tempkin and Pyzhev, 1940):

$$q_e = B_T \ln k_T + B_T \ln c_e \quad \text{Eq. (9)}$$

Where B_T = RT/b is constant related to heat of sorption (J/mol), T is the absolute temperature (K), R is the ideal gas constant 8.314 (J/mol), b is a constant related to the heat of sorption (J/mol) and K_T is the Temkin isotherm constant (l/g). The isotherm constants B_T and K_T are calculated from the slope and intercept of the q_e versus $\ln C_e$. Temkin isotherm equation assumes that the heat adsorption of all the molecules in the layer decreases linearly with coverage of molecules due to the adsorbate-adsorbate repulsions and the adsorption of adsorbate is uniformly distributed and that the fall in the heat of adsorption is linear rather than logarithmic. Fig 12 illustrated the Temkin model for adsorption process. It is noticeable that adsorption of As (V) ions is more fitted with Temkin model than Cr (VI) ions.

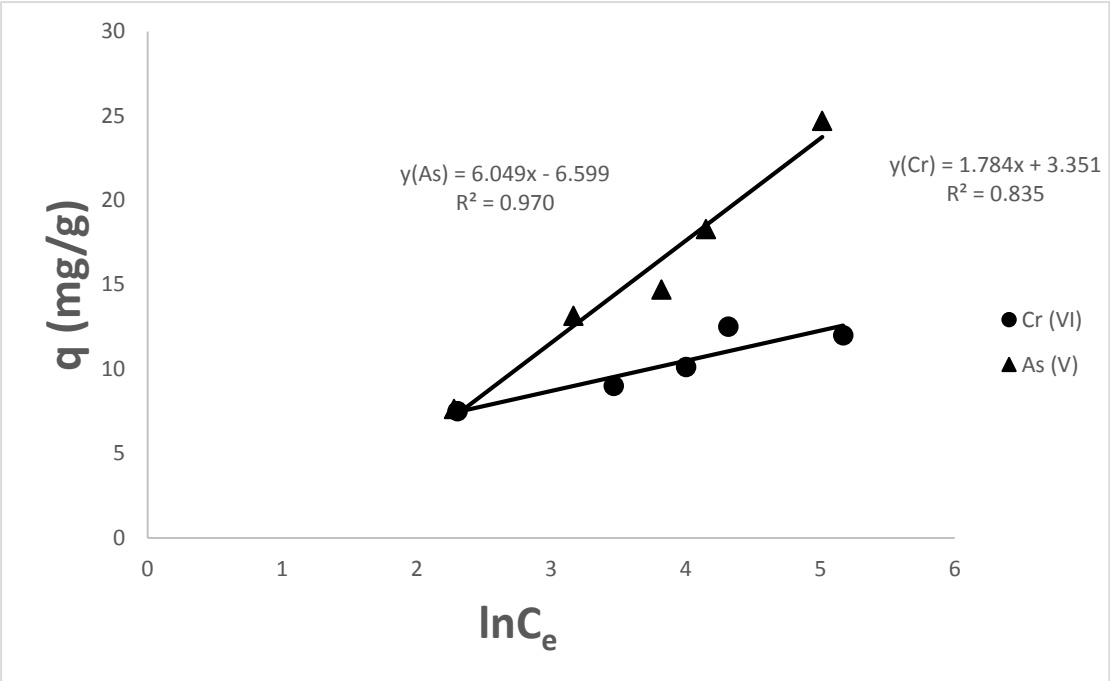

Fig. 12 Temkin plot of Cr (VI) and As (V) ions adsorption on nickel ferrite

3.6.4. Dubinin–Radushkevich isotherm model

The Dubinin-Radushkevich (D-R) isotherm (Shin et al., 2007) was also employed to determine the type of adsorption mechanism (chemical or physical). The linear form of Dubinin-Radushkevich isotherm is expressed as follows:

$$lnq_e = lnq_{DR} - \beta\varepsilon^2 \qquad Eq.\ (10)$$

Where (q_{DR}) is the Dubinin-Radushkevich monolayer capacity (mol/g), (β) is a constant of adsorption energy (mol^2/J^2), and (ε) is the Polanyi potential (Bulut and Tez, 2007) which is related to the equilibrium concentration as follows:

$$\varepsilon = RTln\left(1 + \frac{1}{C_e}\right) \qquad \text{Eq. (11)}$$

By plotting a relationship between lnq_e and ε^2, β and q_{DR} can be obtained for both Cr (VI) and As (V) ions. (D-R) isotherm parameter β used to determine adsorption energy E (KJ/mol) as follows:

$$E = \frac{1}{\sqrt{2\beta}} \qquad \text{Eq. (12)}$$

It is obvious that (D-R) isotherm model is more fitted for As (V) than Cr (VI) so the adsorption energy is 11.1 KJ/mol for As (V) which is indication for chemical sorption. (D-R) isotherm parameters are presented in Table 2.

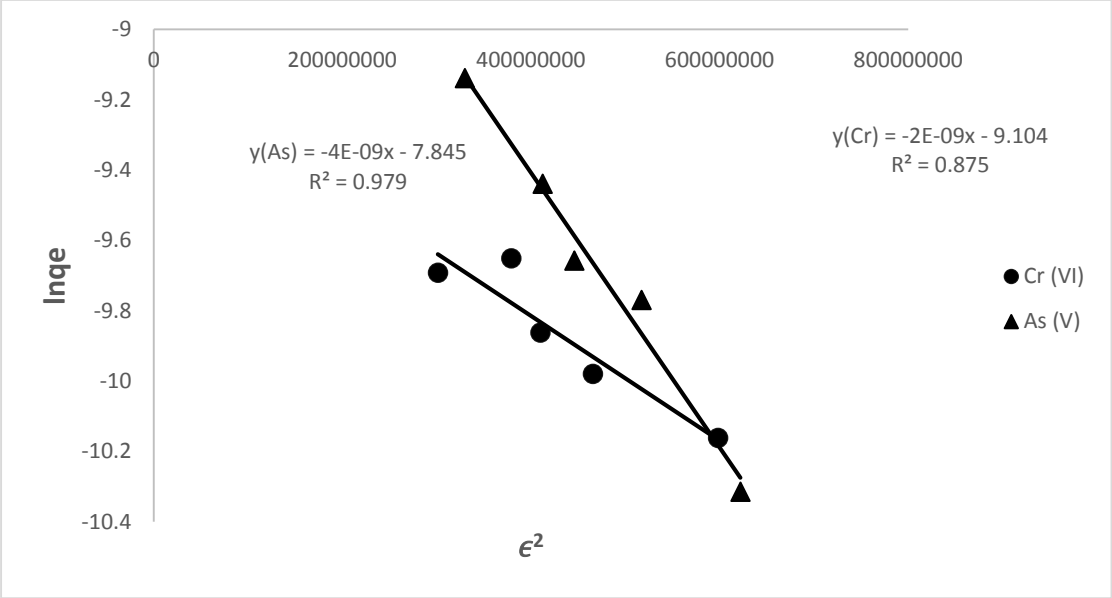

Fig. 13 (D-R) isotherm plot of Cr (VI) and As (V) ions adsorption on nickel ferrite

3.6.5. Flory–Huggins isotherm model

This model gives indication about the degree of surface coverage (θ) and spontaneity of adsorption process (Horsfall and Spiff, 2005). The linear form of Flory–Huggins isotherm model as follows:

$$ln\frac{\theta}{C_0} = lnK_{FH} + n_{FH}ln\,(1-\theta) \qquad \text{Eq. (13)}$$

Where K_{FH} is Flory–Huggins model equilibrium constant, n_{FH} is the Flory–Huggins model exponent and $\theta = (1-C_e/C_o)$ is degree of surface coverage.

The Gibbs free energy of spontaneity (ΔG^o) is calculated from the following equation:

$$\Delta G° = -RTlnK_{FH} \qquad \text{Eq. (14)}$$

For Cr (VI) ΔG^o equal to 18.1 KJ/mol and for As (V) is 18.9 KJ/mol which indicate that sorption process is spontaneous one. Flory–Huggins model parameters are presented in Table 2.

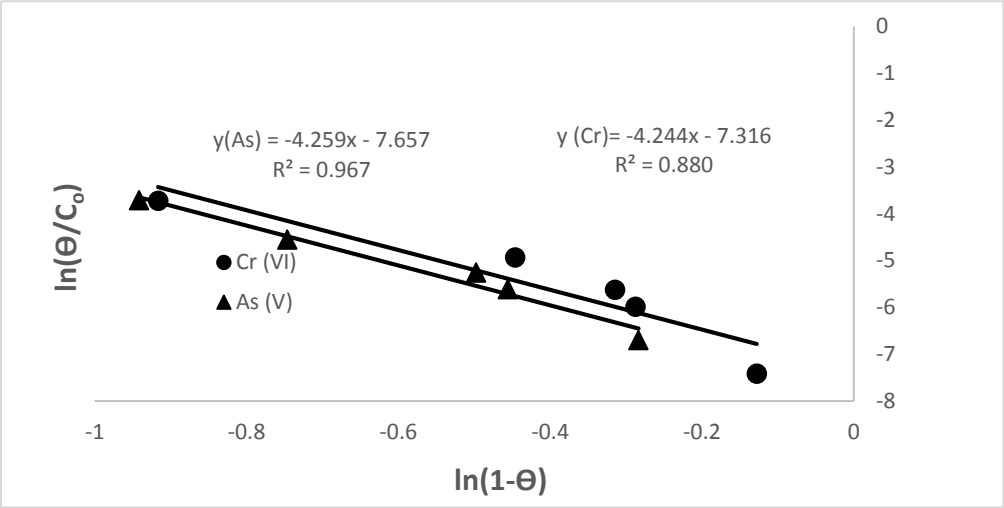

Fig. 14 Flory–Huggins isotherm plot of Cr (VI) and As (V) ions adsorption on nickel ferrite

Table 2. Isotherms constants and correlation coefficients of Cr (VI) and As (V) ions adsorption onto nickel ferrite

Model	Factor	Cr (VI)	As (V)
Langmuir	q_{max} mg/g	12.7	29.7
	K_L L/mg	0.01	0.028
	R^2	0.99	0.98
Freundlich	K_f mg/g	4.94	3.14
	N	5.46	2.4
	R^2	0.86	0.97
Temkin	K_T L/g	1.87	0.33
	B_T J/mol	1.78	6.05
	R^2	0.83	0.97
Dubinin–Radushkevich	β mol^2/J^2	2×10^{-9}	4×10^{-9}
	q_{DR} mg/g	21.6	90
	E KJ/mol	15.8	11.1
	R^2	0.88	0.97
Flory–Huggins	n_{FH}	-4.24	-4.26
	K_{FH}	1510.2	2121.7
	ΔG^o KJ/mol	-18.1	-18.9
	R^2	0.88	0.96

3.7. Characterization of nickel ferrite

The chemical analysis of as-prepared nickel ferrite is proceeded by using inductive coupled plasma optical emission spectroscopy (ICP-OES) after dissolution nickel ferrite in hydrochloric acid. The results of analysis are shown in Table 3.

Table 3. Weight percent of nickel ferrite by ICP-OES

sample	Weight %			
	Fe	Ni	Zn	Mn
Nickel ferrite	50	22.5	< 0.1	< 0.1

The XRD patterns of nickel ferrite nanoparticles prepared by hydrothermal method is shown in Fig. 15. As seen, the most dominant diffraction peaks indicated to the 222, 311, 400, and 511 lattice planes of spinal $NiFe_2O_4$, at 2θ of 30.15°, 35.6°, 43.3° and 57.2°, respectively. There are broadening in diffraction peaks demonstrating the nanostructure of prepared $NiFe_2O_4$.

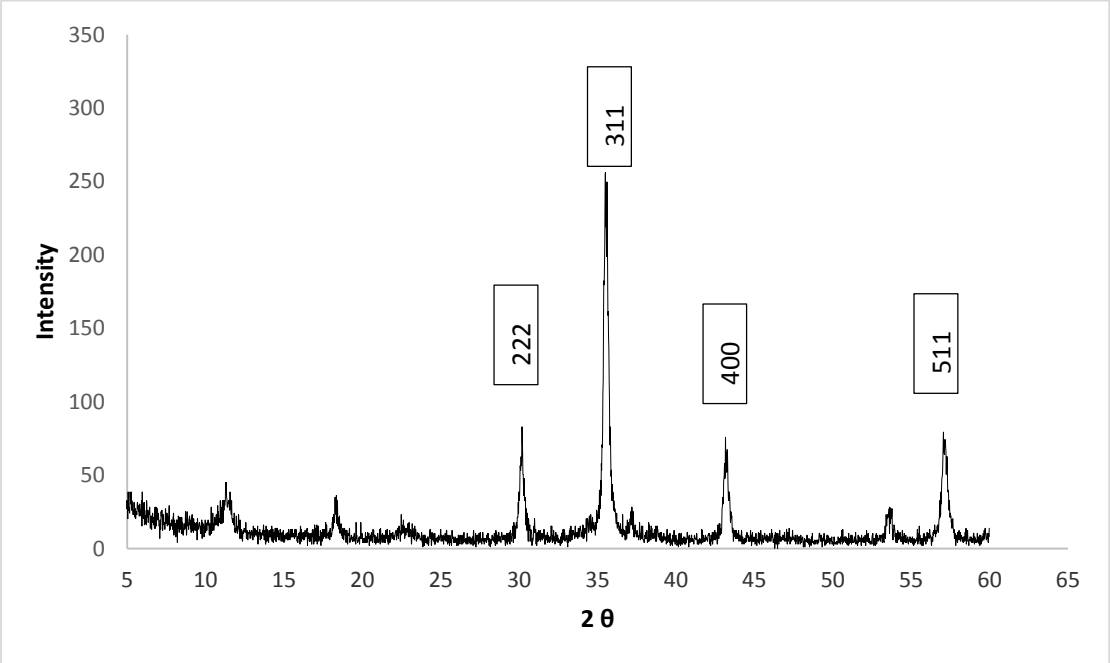

Fig. 15 XRD pattern of prepared nickel ferrite

4. Conclusion

The removal of Cr (VI) and As (V) ions from wastewater by spinel nickel ferrite is studied under different conditions. For Cr (VI) ions, maximum removal reached to 60% after 90 minutes at pH 5, dose of ferrite of 2 g/L and concentration of Cr (VI) ion is 25 mg/L. the adsorption of Cr (VI) ions follows pseudo first order kinetics reaction. Both Weber and Boyd kinetics models are fitted with data so intraparticle and mass transfer are involved in adsorption process. Isotherm data treatment indicate that Langmuir model is well fitted (R^2=0.99). Flory–Huggins model is also applied with R^2=0.88 and ΔG^o equals to -18.1 KJ/mol which indication for spontaneous adsorption process.

For As (V) ions, maximum removal reached to 75% after 90 minutes at pH 5, dose of ferrite of 1 g/L and concentration of As (V) ions is 25 mg/L. the adsorption process follows pseudo second order kinetics reaction. Weber kinetic model (R^2=0.89) is more fitted than Boyd plot (R^2 = 0.69). Both Langmuir and Freundlich isotherm models are well fitted with R^2=0.98 and R^2=0.97, respectively. D-R model is applied with R^2=0.98 and energy of adsorption equals to 11.1 KJ/mol which indication for chemical adsorption. Flory–Huggins model is also applied with R^2=0.97 and ΔG^o equals to -18.9 KJ/mol, which indication for spontaneous adsorption process. Finally, nickel ferrite has more adsorptive capacity for As (V) rather than Cr (VI). Conclusively, nickel ferrite can be used as cost effective adsorbent for metals decontamination from wastewater.

References

- Ajmal M, Rao RAK, Ahmad R, Ahmad J and Rao LA. 2001. Removal and recovery of heavy metals from electroplating wastewater by using kyanite as an adsorbent. J. Hazard. Mater. 87, 127-137
- Al-Mayman SI and Al-Zahran, SM. 2003. Catalytic cracking of gas oils in electromagnetic fields: reactor design and performance. Fuel Process. Technol. 80, 169–182.
- Azizian S. 2004. Kinetic models of sorption: a theoretical analysis. J. Colloid Interface Sci. 276, 47–52.

- Benrabaa R, Boukhlouf H, Löfberg A, and Rubbens A. 2012. Nickel ferrite spinel as catalyst precursor in the dry reforming of methane: synthesis, characterization and catalytic properties. J. Nat. Gas. Chem. 21, 595–604.
- Brown PA, Gill SA and Allen SJ. 2000. Metal removal from wastewater using peat. Water Res. 34, 3907-3916.
- Bulut Y and Tez Z. 2007. Adsorption studies on ground shells of hazelnut and almond J. Hazard. Mater. 149, 35-41.
- Dixit G, Singh JP and Srivastava RC. 2010. Structural and magnetic behavior of NiFe2O4 thin film grown by pulse laser deposition. Indian J. Pure Appl. Phys. 48, 287–291.
- Freundlich HMF. 1906. Over the adsorption in solution. J. Phys. Chem. 57, 385–471.
- Gupta VK, Mittal A, Gajbe V and Mittal J. 2008. Adsorption of basic Fuchs in using waste materials-bottom ash and deoiled soya as adsorbents. J. Colloid Interface Sci. 319, 30–39.
- Horsfall M and Spiff I. 2005. Equilibrium sorption study of Al3+, Co2+, Ag+ in aqueous solution by fluted pumpkin (Telfairia occidentialis HOOK f) waste biomass. Acta. Chim. Slov. 52, 174–181.
- Houlding TK, chabanenko KT and Rahman MT. 2013. Direct amide formation using radiofrequency heating. Org. Biomol. Chem. 11, 4171–4177.
- Kang D, Yu X, Ge M and Song W. 2015. One-step fabrication and characterization of hierarchical MgFe2O4 microspheres and their application for lead removal. Micropor. Mesopor. Mat. 207, 170-178.
- Khenifi A, Zohra B, Kahina B, Houari H and Zoubir D. 2009. Removal of 2, 4-DCP from wastewater by CTAB/bentonite using one-step and two-step methods: a comparative study J. Chem. Eng. Jpn. 146, 345–354.
- Langmuir I. 1916. The constitution and fundamental properties of solids and liquids. Part I. solids. J. Am. Chem. Soc. 38, 2221–2295.
- Malamis S and Katsou E. 2013. A review on zinc and nickel adsorption on natural and modified zeolite, bentonite and vermiculite: examination of process parameters, kinetics and isotherms. J. Hazard. Mater. 252, 428-461.

- Mandal BK and Suzuki KT. 2002. Arsenic round the world: a review. Talanta. 58, 201-235.
- Mohan D and Pittman CU. 2007. Arsenic removal from water/wastewater using adsorbents-a critical review. J. Hazard. Mater. 142, 1–53.
- Selvaraj K, Manonmani S and Pattabhi S. 2003. Removal of hexavalent chromium using distillery sludge. Bioresour. Technol. 89, 207-211.
- Shin EW, Karthi KG and Tshabatala MA. 2007. Adsorption mechanism of cadmium on juniper bark and wood. Bioresour. Technol. 98, 588-594.
- Tempkin MJ and Pyzhev V. 1940. Kinetics of ammonia synthesis on promoted iron catalysts. Acta Physicochim. 12, 217–256.
- Wan-Ngah WS, Kamari A and Koay YJ. 2004. Equilibrium and kinetics studies of adsorption of copper (II) on chitosan and chitosan/PVA beads. Int. J. Biol. Macromol. 34, 155–161.
- Weber WJ and Morris JC. 1963. Kinetics of adsorption on carbon solution. J. Sanit. Eng. Div. Am. Soc. Civil Eng. 89, 31–59.